Buenos Aires – 5 to 9 September 2016
Acoustics for the 21st Century…

PROCEEDINGS of the 22nd International Congress on Acoustics

Materials for Noise Control: Paper ICA2016-597

Adaptive acoustic metasurfaces for the active sound field control

Kateřina Steiger[(a)], Pavel Mokrý[(b)], Jan Václavík[(b)], Pavel Psota[(a)], Roman Doleček[(a)], David Vápenka[(a)], Jakub Nečásek[(b)], Zbyněk Koldovský[(b)]

[(a)] Regional Center for Special Optics and Optoelectronic Systems (TOPTEC), Institute of Plasma Physics AS CR, Za Slovankou 1782/3, 18200 Prague 8, Czech Republic, steigerk@ipp.cas.cz
[(b)] Institute of Mechatronics and Computer Engineering, Technical University of Liberec, Studentská 2, 46117 Liberec, Czech Republic, pavel.mokry@tul.cz

Abstract

Active acoustic metasurfaces (AAMSs) have been recently recognized as very efficient sound shielding structures, which can have large lateral dimensions perpendicular to the direction of the sound wave propagation but very short lateral dimension along the direction of the sound wavevector. The sound shielding principle of AAMSs is based on control of the specific acoustic impedance (SAI). This is achieved by means of an active tuning of elastic properties of piezoelectric transducers, which, therefore, represent the core element of the AAMSs. Using this approach, it is possible to actively control the acoustic coefficients of transmission and reflection of AAMSs. An important point, which has been recently discovered, is the fact that the great suppression of the transmission coefficient can be achieved in the regime, when the SAI of the AAMS is negative. The function of the AAMS in varying operational conditions or in a wide frequency range, however, put delicate stability conditions on the negative values of SAI. In order to keep the AAMS in the stable operation, a concept of adaptive acoustic metasurfaces (AdAMSs) is introduced in this paper. Methods for the real-time estimation and the active control of the SAI values of the AdAMSs are presented. It is shown that the accurate control of the distribution of the SAI on the surface of the AdAMS enables to control the transmitted sound field not only in the magnitude but also in the direction of the transmitted sound wave.

Keywords: Adaptive acoustic metasurfaces; Active sound field control

Adaptive acoustic metasurfaces for the active sound field control

1 Introduction

It is a well-known fact that glass windows and facades, car chassis, airplane fuselages and similar large planar structures have usually a low sound shielding efficiency due their low mass density and low flexural rigidity. An increased noise level in urban areas represents an everlasting environmental problem with severe deteriorating effects on human health. Therefore, the requirement for noise shielding is presently the main subject of environmental noise management. The absolute elimination of all sounds is not trivial, but with the use of novel technologies one can develop efficient tools for a delicate control of a sound wave propagation in an open space. Such tools can be developed using a sophisticated control of the sound transmission through acoustic interfaces.

The efficient control of the sound field and of propagation of sound waves requires very special values of acoustical parameters of the acoustic interfaces, which are not observed in nature. Such artificially fabricated devices are called acoustic metamaterials (AMM) [6, 4, 13, 1]. In our work the attention will be focused on a special form of AMMs that constitute a planar interface between two acoustic media. In 2011, such a form of acoustic metamaterials was for the first time called acoustic metasurface (AMS) [2]. Since that time, several implementations of AMSs have been presented in [7, 17, 18, 5]. A common disadvantage of all aforementioned AMSs is their complicated geometrical structure in the subwavelength dimensions that requires advanced micro-machining technologies of fabrication. Therefore, in the current state of the art there exists a great demand for active AMSs (AAMSs) which do not require advanced fabrication technologies but have acoustic properties comparable to common passive AMSs.

In our work, the novel family of AMSs based on the semi-active approach is discussed. We demonstrate a noise shielding using an AAMS with electronically tunable specific acoustic impedance (SAI) using flexible piezoelectric transducers. The AAMS consists of a curved glass plate with attached piezoelectric Macro Fiber Composite (MFC) actuators shunted by negative capacitor (NC) circuits. Using this approach, which is called active elasticity control (AEC) [3], it is possible to electronically control the effective elasticity of the MFC actuators and, therefore, the flexural rigidity of the whole composite structure of the AAMS. The analysis of the functionality of the proposed noise shielding device was presented in [12] and the detailed numerical model of all material parameters of used MFC actuators was performed in [16]. The noise shielding device has been successfully fabricated and its function has been tested by means of the measurements of frequency dependence of SAI [9]. The pressure difference at the opposite sides of the AAMS has been measured using two microphones. The vibration displacement amplitude on the surface of the AAMS has been measured using frequency-shifted digital holography method. The velocity on the AAMS surface has been measured using laser Doppler vibrometer. Recently, it was discovered that the great suppression of the noise through the AAMS can be achieved in the regime of the negative SAI of the AAMS [10].

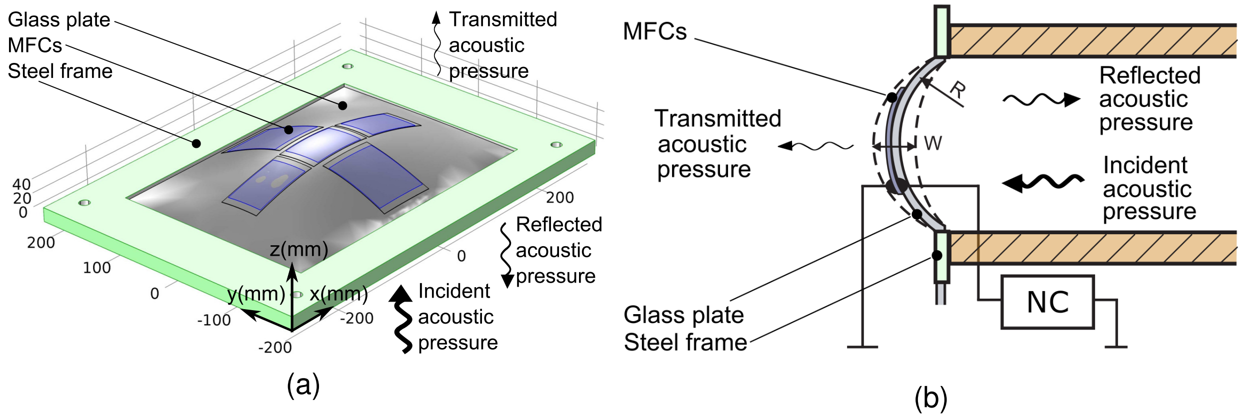

Figure 1: **Considered sound shielding system, which consists of the curved glass plate fixed in a rigid steel frame at its edges and with piezoelectric MFC actuators attached. An incident sound wave of the acoustic pressure strikes the glass plate. It makes the glass plate vibrate and a part of the sound wave is reflected and a part is transmitted. (a) 3-D; (b) 2-D cross-section with the shunted electronic circuit with a negative capacitance.**

In varying operational conditions or in a wide frequency range, however, this regime puts delicate stability conditions on the negative values of SAI. In order to keep the AAMS in a stable operation, a concept of adaptive acoustic metasurfaces (AdAMSs) is introduced.

2 Noise shielding by means of the active acoustic metasurface

In this section, a brief explanation of noise shielding principles using AAMS is presented. Our implementation of the noise shielding device based on the AAMS is shown in Fig. 1. It consists of a curved glass plate of the thickness $h_g = 4$ mm. The curved glass plate is fixed at its edges in a rigid steel frame of inner dimensions $a = 42$ cm and $b = 30$ cm and placed onto the acoustic box where the source of the incident sound is situated. On the top surface of the glass plate, piezoelectric Macro Fiber Composite (MFC) actuators of the thickness $h_{\mathrm{MFC}} = 300$ μm are attached. The composite structure of the curved glass with the MFC actuators creates an interface between two acoustic media of air. An incident sound wave of the acoustic pressure strikes the glass plate. It makes the glass plate vibrating. A part of the sound wave is reflected while the other part is transmitted.

The analysis performed by Novakova et al. [12] on the analytical model of the generally curved rectangle glass shell indicated the crutial role of curvature and in-plane stiffness of the AAMS on its sound shielding efficiency. These analytical estimations have been confirmed by numerical simulations presented in the same article. With a non-zero shell curvature, the acoustic transmission through the plate decreases. This actually means that a greater part of the incident sound wave energy is reflected. Moreover, the additional layer of the MFC actuators on the glass plate gives rise to an active part of the AAMS structure. The actuators are connected in parallel to the electronic circuit with a negative capacitance (NC), as it is shown in Fig. 1(b).

This controls their elastic properties and, therefore, the sound transmission through the whole structure of the AAMS.

2.1 Acoustic transmission loss

It is known that the transmission of sound waves through an interface between two different acoustic media is controlled by a physical property called specific acoustic impedance (SAI) z_m. In the case of a planar structure, also the considered AAMS, the value of the SAI (in Pa s m^{-1}) is defined as a ratio of the acoustic sound pressure p over the particle velocity v:

$$z_m = p/v, \tag{1}$$

where $p = p_i + p_r - p_t$, p_i is the incident acoustic pressure, p_r is the reflected acoustic pressure and p_t is the transmitted acoustic pressure. It is convenient to express the amount of transferred acoustic potential energy by introducing the physical quantity called acoustic transmission loss (TL). This is defined as a ratio of the acoustic powers of the incident and transmitted acoustic waves (usually expressed in dB). According to [8] it is possible to express the TL in terms of the SAI z_m of the interface between two acoustic media, i.e. the noise shielding device:

$$\mathrm{TL} = 20 \log_{10} \left| 1 + \frac{z_m}{2 z_a} \right|, \tag{2}$$

where $z_a = \varrho_0 c$ is the characteristic acoustic impedance of air, ϱ_0 is the air density and c is the sound velocity in the air.

It can be seen from Eq. (2) that large values of the TL correspond to large values of the SAI z_m. Using the AAMS it is possible to increase the value of z_m to a great extent while keeping the weight of the structure as small as possible.

2.2 Active elasticity control

Recently, the analytical formula for the SAI of the generally curved glass shell of a rectangular shape has been presented in [12]. According to this analysis, the SAI z_m of the considered noise shielding plate can be approximated by the formula:

$$z_m(\omega) \approx \frac{i\pi^2 \left(h_g + h_{\mathrm{MFC}}\right)}{16\,\omega} \left[\varrho\omega^2 - \left(\xi Y + \zeta G\right) \left(1 + \frac{i}{Q_m}\right) \right], \tag{3}$$

where

$$\xi = \frac{2\nu\xi_x\xi_y + \xi_x^2 + \xi_y^2}{1-\nu^2}, \tag{4}$$

$$\zeta = \frac{\pi^4 \left(a^2+b^2\right)^2}{a^4 b^4 \left(h_g + h_{\mathrm{MFC}}\right)}, \tag{5}$$

$$Y = \frac{Y_g h_g + Y_{\mathrm{MFC}} h_{\mathrm{MFC}}}{h_g + h_{\mathrm{MFC}}}, \tag{6}$$

$$G = \frac{Y_g^2 h_g^4 + Y_{\mathrm{MFC}}^2 h_{\mathrm{MFC}}^4 + 2 Y_g Y_{\mathrm{MFC}} h_g h_{\mathrm{MFC}} \left(2h_g^2 + 3 h_g h_{\mathrm{MFC}} + 2 h_{\mathrm{MFC}}^2\right)}{12\left(1-\nu^2\right)\left(Y_g h_g + Y_{\mathrm{MFC}} h_{\mathrm{MFC}}\right)}. \tag{7}$$

Symbols ν, ρ, and Q_m are the average Poisson ratio, mass density, and mechanical quality factor of the noise shielding device. Symbols ξ_x and ξ_y stand for the average inverse radii of curvature of the glass shell along the x and y coordinates, respectively. Symbols Y_g and Y_{MFC} stand for the Young's modulus of the glass plate and for the piezoelectric MFC actuator. Symbol ω is the angular frequency of the incident sound wave, and $i = \sqrt{-1}$.

It immediately follows from Eqs. (3), (6) and (7) that when the value of Y_{MFC} is increased, the effective values of the Young's modulus Y and the bending stiffness coefficient G of the whole structure are increased as well. Therefore, the large values of z_m can be achieved by increasing the Young's modulus of the MFC actuator using the active elasticity control (AEC) method.

The AEC method has been developed by Date et al. [3] to control the elastic properties of piezoelectric actuators by connecting them to active shunt circuits. The principle of the AEC method can be understood by writing down the equations of state for the strain S_1 and electric displacement D_3 in the piezoelectric actuator shunted by the external capacitor C:

$$S_1^{(c)} = (1/Y_S)\,T_1 + d_{31}\,(V_c/h_e), \tag{8}$$

$$D_3^{(c)} = d_{31}\,T_1 + \varepsilon_{33}\,(V_c/h_e), \tag{9}$$

$$D_3^{(c)} = -C\,V_c/A_e. \tag{10}$$

Symbol T_1 is the in-plane mechanical stress; V_c stands for the voltage on the electrodes of piezoelectric actuator shunted by the external capacitance C. Symbols Y_S, d_{31}, and ε_{33} stand for the Young's modulus with short-circuited electrodes, piezoelectric coefficient and permittivity of the piezoelectric actuator. Symbols A_e and h_e stand for the macroscopic values of the area of electrodes and distance between electrodes, respectively. The capacitance of the piezoelectric actuator is equal to $C_S = \varepsilon_{33}\,A_e/h_e$. The macroscopic value of the Young's modulus of the piezoelectric MFC actuator, which is shunted by the external capacitor with capacitance C, is given by $Y_{\mathrm{MFC}} = T_1/S_1^{(c)}$. The value of Y_{MFC} can be readily expressed from Eqs. (8)-(10) as follows:

$$Y_{\mathrm{MFC}} = \frac{T_1}{S_1^{(c)}} = Y_S\left(\frac{1+\alpha}{1-k^2+\alpha}\right), \tag{11}$$

where $k^2 = d_{31}^2 Y_S/\varepsilon_{33}$ is the electromechanical coupling factor of the piezoelectric actuator, and $\alpha = C/C_S$.

It follows from Eq. (11) that the required large values of the z_m of the AAMS, i.e. large values of the Y_{MFC}, can be achieved when the value of external capacitance C is close to the value:

$$C \to -(1-k^2)\,C_S. \tag{12}$$

It means that the effective value of the shunt capacitance has to be negative. For this purpose, the active circuit, which is called the negative capacitor (NC), has been suggested as an external shunt circuit to the MFC actuators. The electrical scheme of the NC circuit is shown in Fig. 2. It is possible to adjust the resistances R_0 and R_1 in such a way that the real and imaginary parts of the NC circuit capacitance C satisfy the condition given by Eq. (12). In

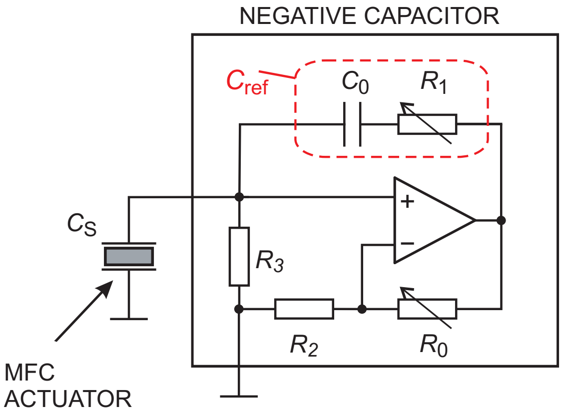

Figure 2: **Electrical scheme of the equivalent circuit of the synthetic impedance connected to the MFC actuators in our noise shielding device. The resistances R_0 and R_1 are adjustable.**

order to precisely control the parameters of the NC circuit electronically, the digital synthetic impedance has been constructed [11] and implemented in the AAMS. The capacitance of the NC equivalent circuit is equal to:

$$C = -\frac{R_0}{R_2}\left(\frac{C_0}{1 + i\omega C_0 R_1}\right) - \frac{i}{\omega R_3}. \tag{13}$$

It is seen that the capacitance of the negative capacitor is a function of the frequency ω of the incident sound wave. The absolute value and argument of the negative capacitor capacitance can be adjusted by adjustable resistors R_0 and R_1. The other circuit parameters C_0, R_2, and R_3 are constant.

In order to maximize the TL through the AAMS, it is necessary to achieve the maximal value of the effective Young's modulus of the MFC actuators Y_{MFC} attached to the curved glass plate. We consider a frequency-independent complex value of the capacitance of the MFC actuator,

$$C_s = C_s' \left(1 - i \tan \delta_s\right), \tag{14}$$

where C_s' and $\tan\delta_s$ are, the real part of the capacitance and the dielectric loss tangent of the piezoelectric actuator, respectively. The optimal adjustment of the NC circuit parameters R_0 and R_1 can be computed using Eqs. (11), (12), (13), and (14). Let us consider the frequency of the first resonance mode of the AAMM to be $f = 300$ Hz. Next, let the Young's modulus be $Y_S = 3.26 \times 10^{10}$ Pa, mechanical quality factor $Q_m = 31.3$, capacitance $C_s' = 2.070$ μF, and loss tangent $\tan\delta_s = 0.015$ of the piezoelectric MFC actuator. Let the fixed parameters of the NC circuit be $C_0 = 500$ nF, $R_2 = 1$ kΩ, and $R_3 = 500$ MΩ, and the square of the effective electromechanical coupling factor of the whole AAMM be $k_{31}^2 = 0.54$. Figures 3(a) and (b) show the contour plots of the computed absolute value (a) and argument (b) of the inverse of the effective Young's modulus of the piezoelectric actuator, i.e. $1/Y_{\mathrm{MFC}}$, as functions of the

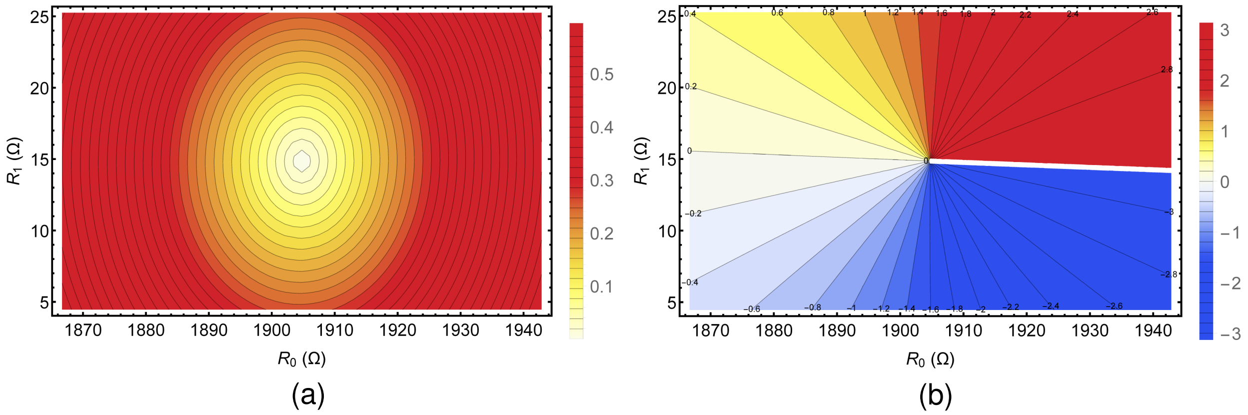

Figure 3: **Contour plots of absolute value (a) and argument (b) of the inverse of the effective Young's modulus Y_{MFC} of the piezoelectric MFC actuator shunted by the negative capacitor shown in Fig. 2 as functions of the resistances R_0 and R_1.**

values of circuit parameters R_0 and R_1 of the NC. It is seen that the inverse absolute value of the effective Young's modulus of the MFC actuators, i.e. $\mathrm{Abs}(1/Y_{\mathrm{MFC}})$, approaches zero at $R_0 = 1904.77\ \Omega$ and $R_1 = 14.86\ \Omega$. In addition, it is seen that the argument of the effective Young's modulus of the MFC actuators, i.e. $\mathrm{Arg}(1/Y_{\mathrm{MFC}})$, represents a monotonic function along a circle with the center in the optimal adjustment.

Although the above description of the sound shielding system suggests a straightforward adjustment of the NC circuit, its practical implementation experiences considerable difficulties. The reason is that the optimal adjustment of the NC circuit given by Eqs. (12) has to be satisfied with a high accuracy. Sluka et al. [14] have estimated that the relative deviation of the NC circuit capacitance from its proper value must be smaller than 0.1%. This greatly narrows the region of the NC circuit capacitances, where the required values of Y_{MFC} can be achieved.

In addition, it is quite difficult to satisfy the optimal adjustment of the NC with fixed values of R_0 and R_1 in varying operational conditions. To overcome this drawback, we can use the idea of the iterative adaptive algorithm developed earlier by Sluka et al. [14]. This algorithm is based on the property of monotonicity in the $\mathrm{Arg}(1/Y_{\mathrm{MFC}})$ with respect to the values of R_0 and R_1, which is presented in Fig. 3(b).

3 Concept of adaptive acoustic metasurfaces

In order to keep the AAMS working in varying operational conditions, a concept of adaptive acoustic metasurfaces (AdAMSs) is introduced in this work. It is seen in Fig. 3 that if the value of $\mathrm{Arg}(1/Y_{\mathrm{MFC}})$ in a slightly untuned AAMS is known, it is possible to identify the corrections to R_0 and R_1, which yield the optimal adjustment of the NC circuit. Therefore, the key objective is to introduce a way to measure $\mathrm{Arg}(1/Y_{\mathrm{MFC}})$ in a real system. One possibility has been introduced earlier by means of the error microphones [14], which is not the preferred option, because additional electronics are needed. The construction of our AAMS enables to attach

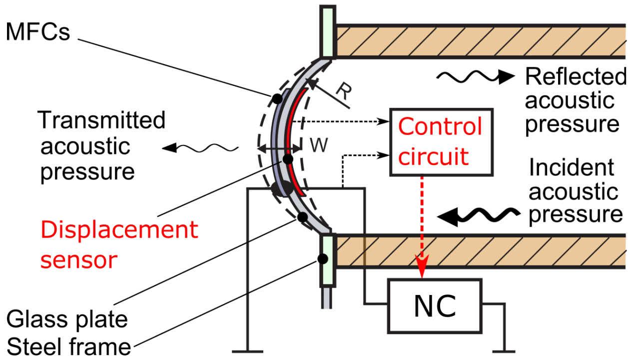

Figure 4: **Scheme of the developed sound shielding system based on the adaptive AAMS. A displacement sensor is implemented by means of the second set of MFC actuators attached to the curved glass surface. The electric output signal from these MFC actuators corresponds to the normal displacement of the curved glass surface. This signal is introduced to the control circuit, which adjusts the values of the NC circuit parameters R_0 and R_1 according to the iterative algorithm.**

the second set of MFC actuators to the inner side of the glass plate, much smaller in the size then the active MFC actuators on the outer side, and use them as a strain sensor (MFC-SS).

Fig. 4 shows the scheme of the developed sound shielding system based on the AdAMS. The output electric signal V_s from the MFC-SS is proportional to the strain S_1 in the shunted MFC actuators. Since the value of the strain S_1 in the shunted MFC actuators is nearly zero in the slightly untuned AAMS, it follows from Eq. (8) that $T_1 \propto -V_c$. It means that the in-plane stress T_1 in the shunted MFC actuator is proportional to the voltage V_c, which is applied back from the NC. It means that the inverse value of the effective Young's modulus of the NC shunted MFC capacitor, i.e. $1/Y_{\mathrm{MFC}} = S_1^{(c)}/T_1$, can be estimated from the ratio V_s/V_c. In addition, the argument $\mathrm{Arg}(1/Y_{\mathrm{MFC}})$ is equal to $\mathrm{Arg}(V_s) - \mathrm{Arg}(V_c)$. Using this approach, the argument of the inverse value of the effective Young's modulus of the MFC actuator, which is shunted by the NC, can be measured with a high precision using the electrical signals in the AdAMS system. When the value of $\mathrm{Arg}(1/Y_{\mathrm{MFC}})$ is known, the corrections to the values of R_0 and R_1 can be identified using the data presented in Fig. 3. As a result, this procedure makes it possible to keep the proper adjustment of the resistors R_0 and R_1 in the NC circuit according to the condition given by Eq. (12).

4 Conclusions

The noise shielding device, which is based on the adaptive acoustic metasurfaces (AdAMS), has been developed and theoretically analyzed. The AdAMS consists of the curved glass plate with attached piezoelectric Macro Fiber Composite (MFC) actuators connected to the negative capacitance (NC) circuit. Using the proper adjustment of the electronic components in the NC circuit, it is possible to achieve a great increase in the acoustic transmission loss of the sound transmitted though the AdAMS. Despite its simple principle and construction, the practical implementation of the sound shielding system suffers severe difficulties. These difficulties are caused by the requirement of an extremely accurate adjustment of the NC circuit, whose capacitance must precisely match the capacitance of the piezoelectric MFC actuator. It is obvious that, in the varying operational conditions, such a capacitance matching cannot be kept with a fixed adjustment of parameters R_0 and R_1 in the NC circuit. In order to overcome this problem, the precise electronic feedback control of values R_0 and R_1 in the NC circuit has been implemented in the AdAMS. The feedback control is based on the approximate measurement of the $\mathrm{Arg}(1/Y_{\mathrm{MFC}})$ of the piezoelectric MFC actuator. The value of $\mathrm{Arg}(1/Y_{\mathrm{MFC}})$ is estimated from the MFC displacement sensor, which is implemented in the AdAMS by means of the MFC sensors attached to the surface of the AdAMS. The iterative algorithm [15] processes the value of $\mathrm{Arg}(1/Y_{\mathrm{MFC}})$ and computes corrections to the values of R_0 and R_1 in the NC circuit, so that the excellent sound shielding efficiency of the AdAMS is achieved even in varying operational conditions.

The suggested system is ready to be assembled and tested in a laboratory.

Acknowledgements

This work was supported by Czech Science Foundation Project No.: GA16-11965S, co-financed from Ministry of Education, Youth and Sports of the Czech Republic in the Project No. NPU LO1206. Authors acknowledge Pavel Márton of the Institute of Mechatronics and Computer Engineering, Technical University of Liberec for his help with development of synthetic shunt impedance circuit.

References

[1] F. Bongard, H. Lissek, and J. R. Mosig. Acoustic transmission line metamaterial with negative/zero/positive refractive index. *Physical Review B*, 82(9):094306, Sept. 2010.

[2] P.-Y. Chen, M. Farhat, S. Guenneau, S. Enoch, and A. Alu. Acoustic scattering cancellation via ultrathin pseudo-surface. *Applied Physics Letters*, 99(19):191913, Nov. 2011. WOS:000297030200028.

[3] M. Date, M. Kutani, and S. Sakai. Electrically controlled elasticity utilizing piezoelectric coupling. *Journal of Applied Physics*, 87(2):863–868, 2000. NIC.

[4] N. Fang, D. Xi, J. Xu, M. Ambati, W. Srituravanich, C. Sun, and X. Zhang. Ultrasonic metamaterials with negative modulus. *Nature Materials*, 5(6):452–456, June 2006. WOS:000237968100016.

[5] S. Lani, K. G. Sabra, and F. L. Degertekin. Modal and transient analysis of membrane acoustic metasurfaces. *Journal of Applied Physics*, 117(4):045308, Jan. 2015. WOS:000348998200056.

[6] J. Li and C. Chan. Double-negative acoustic metamaterial. *Physical Review E*, 70(5):055602(R), Nov. 2004.

[7] G. Ma, M. Yang, S. Xiao, Z. Yang, and P. Sheng. Acoustic metasurface with hybrid resonances. *Nature Materials*, 13(9):873–878, Sept. 2014. WOS:000341343500018.

[8] Z. Maekawa, J. H. Rindel, and P. Lord. *Environmental and Architectural Acoustics*. CRC Press, 2 edition, Feb. 2011.

[9] P. Mokrý, P. Psota, K. Steiger, J. Václavík, R. Doleček, V. Lédl, and M. Šulc. Noise suppression in curved glass shells using macro-fiber-composite actuators studied by the means of digital holography and acoustic measurements. *AIP Advances*, 5(2):027132, Feb. 2015.

[10] P. Mokrý, J. Václavík, J. Nečásek, K. Steiger, P. Psota, and R. Doleček. Noise transmission through active acoustic metamaterials in the negative elasticity regime. In *Proceedings of the 22nd International Congress on Sound and Vibration*, pages 1–8, Florence, Italy, July 2015.

[11] J. Nečásek, J. Václavík, and P. Marton. Digital synthetic impedance for application in vibration damping. *Review of Scientific Instruments*, 87(2):024704, Feb. 2016.

[12] K. Novakova, P. Mokry, and J. Vaclavík. Application of piezoelectric macro-fiber-composite actuators to the suppression of noise transmission through curved glass plates. *IEEE Transactions on Ultrasonics, Ferroelectrics and Frequency Control*, 59(9):2004–2014, Sept. 2012.

[13] P. Sheng, J. Mei, Z. Liu, and W. Wen. Dynamic mass density and acoustic metamaterials. *Physica B: Condensed Matter*, 394(2):256–261, May 2007.

[14] T. Sluka, H. Kodama, E. Fukada, and P. Mokrý. Sound shielding by a piezoelectric membrane and a negative capacitor with feedback control. *IEEE Transactions on Ultrasonics, Ferroelectrics, and Frequency Control*, 55(8):1859–1866, Aug. 2008.

[15] T. Sluka and P. Mokrý. Feedback control of piezoelectric actuator elastic properties in a vibration isolation system. *Ferroelectrics*, 351:51–61, 2007. 8th European Conference on Applications of Polar Dielectrics (ECAPD-8), Metz, FRANCE, SEP 05-08, 2006.

[16] K. Steiger and P. Mokrý. Finite element analysis of the macro fiber composite actuator: macroscopic elastic and piezoelectric properties and active control thereof by means of negative capacitance shunt circuit. *Smart Materials and Structures*, 24(2):025026, Feb. 2015.

[17] Y. Xie, W. Wang, H. Chen, A. Konneker, B.-I. Popa, and S. A. Cummer. Wavefront modulation and subwavelength diffractive acoustics with an acoustic metasurface. *Nature Communications*, 5:5553, Nov. 2014. WOS:000345913600017.

[18] J. Zhao, B. Li, Z. N. Chen, and C.-W. Qiu. Redirection of sound waves using acoustic metasurface. *Applied Physics Letters*, 103(15):151604, Oct. 2013. WOS:000325779700022.